3-14-2001

Magnetic phase diagram of the diluted metamagnet $Fe_{0.95}Mg_{0.05}Br_2$

H. Aruga Katori
RIKEN (The Institute of Physical and Chemical Research), Wako, Saitama, Japan

K. Katsumata
RIKEN (The Institute of Physical and Chemical Research), Wako, Saitama 351-0198, Japan

O. Petracic
Laboratorium fu¨r Angewandte Physik, Gerhard-Mercator-Universita¨t, Duisburg, Germany

Wolfgang Kleemann
Laboratorium fu¨r Angewandte Physik, Gerhard-Mercator-Universita¨t, Duisburg, Germany, wolfgang.kleemann@uni-due.de

T. Kato
Laboratorium fu¨r Angewandte Physik, Gerhard-Mercator-Universita¨t, Duisburg, Germany

See next page for additional authors

Magnetic phase diagram of the diluted metamagnet $Fe_{0.95}Mg_{0.05}Br_2$

H. Aruga Katori and K. Katsumata
RIKEN (The Institute of Physical and Chemical Research), Wako, Saitama 351-0198, Japan

O. Petracic, W. Kleemann, T. Kato,* and Ch. Binek
Laboratorium für Angewandte Physik, Gerhard-Mercator-Universität, D-47048 Duisburg, Germany
(Received 7 June 2000; revised manuscript received 13 November 2000; published 14 March 2001)

The axial magnetic phase diagram of the antiferromagnet $Fe_{0.95}Mg_{0.05}Br_2$ is studied by specific heat, superconducting quantum interference device, and Faraday rotation techniques. The diamagnetic impurities give rise to random-field criticality along the second-order phase line $H_c(T)$ between $T_N = 13.1$ K and a multicritical point at $T_m \approx 5$ K, and to a spin-flop line between T_m and the critical end-point temperature $T_e \approx 3.5$ K. The phase line $H_1(T) < H_c(T)$ ending at T_m is probably due to symmetric nondiagonal exchange.

DOI: 10.1103/PhysRevB.63.132408 PACS number(s): 64.60.Kw, 75.25.+z, 75.30.Kz, 75.50.Ee

The magnetic phase diagram of the antiferromagnetic (AF) insulator $FeBr_2$ has attracted appreciable interest in recent years.[1] It is much more complex than that of the related metamagnet $FeCl_2$.[2,3] In the hexagonal unit cell of $FeBr_2$ [space group $D_{3d}^3 = P\bar{3}m1$, Néel temperature $T_N = 14.1$ K; see Fig. 1(a), inset], adjacent (001) layers of Fe^{2+} ions are separated by two layers of Br^- ions. The spin directions at low temperatures $T \ll T_N$ and in zero external magnetic field H are conventionally assumed to point parallel and antiparallel to [001], respectively, from layer to layer, thus giving rise to a Néel-type ground state with ''up'' and ''down'' spin sublattices as in $FeCl_2$ (space group $D_{3d}^5 = R\bar{3}m$, $T_N = 23.7$ K). However, while $FeCl_2$ reveals a classic tricritical point on its H-T phase line,[2,3] $FeBr_2$ behaves in a more complicated fashion [Fig. 1(a)].

Similarly as in $FeCl_2$, the lines H_{c1} and H_{c2} denote the phase transition of first order from AF long-range order to the paramagnetic (PM) saturated phase via a mixed phase (AF+PM). However, above the multicritical-point (MCP) temperature $T_m = 4.6$ K, apart from the critical phase line $H_c(T)$, regions of strong noncritical fluctuations are encountered. They peak along lines denoted as $H_-(T)$ and $H_+(T)$, respectively.[4] In addition, a first-order phase transition line $H_1(T)$ is revealed by specific heat measurements[5] in the vicinity of $H_-(T)$. Recently,[1] by using neutron scattering transverse AF ordering was observed in both phases AFI and AFII, as depicted schematically in Fig. 1(a) by tilted arrows. The transverse order parameter, which exhibits a peak at $T_1 = T(H_1)$, does not vanish in zero field and vanishes upon approaching the critical line $H_c(T)$. In addition, a weak transverse ferromagnetic (FM) moment, which appears below T_1, is considered as a secondary order parameter of phase AFI.

Since both the experimental data and the theoretical description[6] of $FeBr_2$ are still far from being complete, experiments in order to clarify the situation are necessary. Being an anisotropic Heisenberg model system with a tendency towards transverse spin ordering, it seems interesting to investigate the influence of diamagnetic impurities replacing the Fe^{2+} ions in $FeBr_2$. They are suitable to diminish the anisotropy of the exchange interaction, while the uniaxial single-ion anisotropy should be less affected by ionic replacements. Moreover, they break the translational symmetry and thus allow nondiagonal exchange interaction to become an effective source of transverse spin ordering.[1]

In this paper we present data revealing the effect of Mg^{2+} ions doped at a low level $x = 0.05$. First, the H_1 phase line reappears as in the case of pure $FeBr_2$ (Ref. 1) and seems to

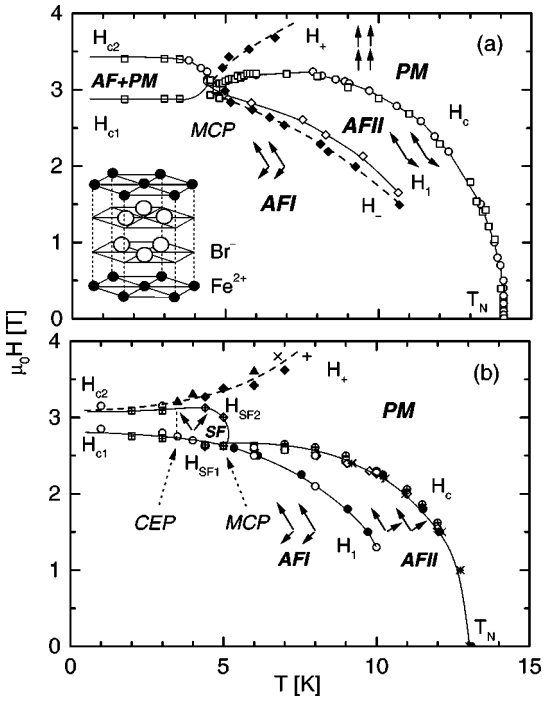

FIG. 1. H-T phase diagrams of $FeBr_2$ (a) and $Fe_{0.95}Mg_{0.05}Br_2$ (b) presented by interpolated lines and data points (see Ref. 1 and text, respectively, for details). H_{c1}, H_{SF1} and H_1 are first-order phase lines with upper boundaries of the corresponding mixed phases, H_{c2} and H_{SF2}, respectively. H_- and H_+ denote the lines of peak positions of noncritical fluctuations. Critical points (CEP and MCP), transition temperatures (T_N), and phases (PM, SF, AFI, and AFII) are indicated (see text). Tentative spin structures referring to adjacent Fe^{2+} layers [inset in (a) shows the unit cell] are schematically sketched by arrows.

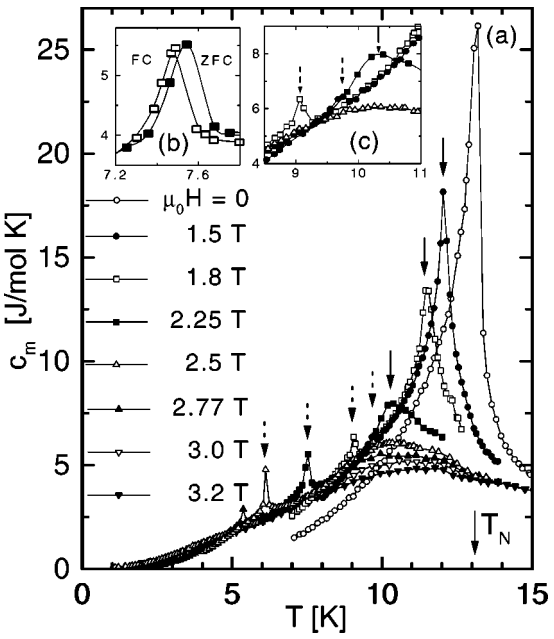

FIG. 2. (a) Magnetic specific heat c_m vs T of $Fe_{0.95}Mg_{0.05}Br_2$ measured at magnetic fields $0 \leqslant \mu_0 H \leqslant 3.2$ T. The transition temperatures T_c and T_1 are indicated by solid and dashed arrows, respectively (see text). The insets (b) and (c) show hysteresis observed at $\mu_0 H = 2.25$ T upon zero-field (ZFC) and field cooling (FC), and an enlarged detail of (a).

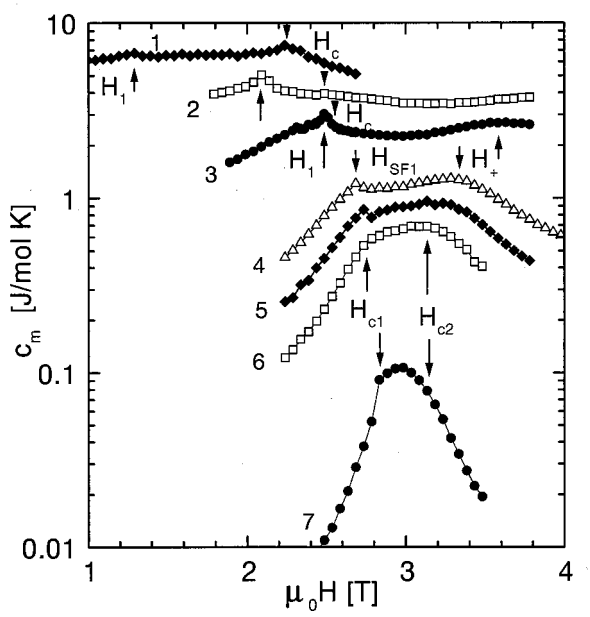

FIG. 3. Semilogarithmic plot of the magnetic specific heat c_m vs H, measured at $T = 10.0$ K (1), 8.0 K (2), 6.0 K (3), 4.0 K (4), 3.5 K (5), 3 K (6), and 1.0 K (7). Phase transition fields H_c, H_1, H_{SF1}, H_{c1}, and H_{c2} and anomalies H_+ are indicated by arrows.

be stabilized by the intentional disorder. Second, the quenched randomness of the magnetic vacancy distribution gives rise to random-field (RF) effects, a well-known phenomenon in dilute uniaxial AF compounds subjected to uniform external axial magnetic fields.[7] Third, spin-flop-like transitions are observed below the multicritical point, where the phase lines H_c and H_1 meet. This feature is discussed in view of the revised spin structure of pure $FeBr_2$,[1] which involves transverse spin components similarly as a classic spin-flop phase.

The experiments were carried out on Bridgman-grown samples with the nominal composition $Fe_{0.95}Mg_{0.05}Br_2$ as-cleft parallel to planes perpendicular to the hexagonal c axis with thickness $t \approx 0.2$ mm and mass $m \approx 8$ mg. Specific heat measurements were performed with an automatic microcalorimeter (Oxford Instruments, MagLab) in applied axial fields up to $\mu_0 H = 4$ T. Magnetometry was performed by means of the superconducting quantum interference device (SQUID) technique (Quantum Design, MPMS 5S) and locally resolved Faraday rotation (FR) in axial magnetic fields up to $\mu_0 H = 5$ T.

Figure 2 shows the temperature dependence of the magnetic specific heat, c_m, for axial magnetic fields $0 \leqslant \mu_0 H \leqslant 3.2$ T after subtracting the diamagnetic lattice background measured separately in zero external field on a sample of $MgBr_2$. At $H = 0$ a large λ-shaped anomaly due to the AF-to-PM phase transition is observed at $T_N = 13.10 \pm 0.05$ K. At $H > 0$ it shifts towards lower temperatures along the phase line $H_c(T)$. While its shape becomes more symmetric at intermediate fields $1.5 \leqslant \mu_0 H \leqslant 1.8$ T, rounding at $\mu_0 H > 2.25$ T indicates the absence of axial long-range order in high enough external fields. A secondary peak emerges at lower temperatures for $\mu_0 H \geqslant 1.5$ T [dashed arrows; see also Fig. 2(c)]. It sharpens at intermediate fields $\mu_0 H \approx 2.5$ T and disappears at $\mu_0 H > 2.8$ T. In analogy to observations[5] made on $FeBr_2$, we attribute this peak to the AFI-to-AFII phase transition. Its position designates the phase line $H_1(T)$, which is plotted together with $H_c(T)$ in Fig. 1(b) (solid circles). The previously conjectured[5] first-order nature of the anomaly at $H_1(T)$ is confirmed by the observation of hysteresis in specific heat data recorded after zero-field cooling (ZFC) and upon field cooling (FC), respectively [Fig. 2(b)].

The phase diagram is complemented by data originating from isotherms c_m vs H [Figs. 3 and 1(b), open circles]. With decreasing T the intensity of the anomaly at H_c becomes gradually transferred to that at H_1 (curves 1–3). This indicates that more and more entropy is spent at the AFI-to-AFII phase transition of the transverse order parameters, while the contribution due to the decay of axial AF order at H_c becomes less important. As shown in Fig. 1(b), the two phase lines $H_1(T)$ and $H_c(T)$ meet at $T_m \approx 5$ K in a multicritical point (MCP).

The single peaks occurring below T_m at $T = 4$ and 3.5 K (curves 4 and 5) denoted as H_{SF1} vanish at the metamagnetic spin-flip line below the critical end-point (CEP) temperature $T_e \approx 3.5$ K (see below). The flat background obeys the Clausius-Clapeyron rule for latent heat, $\delta Q \propto (dH/dT)_{H=H_c}$, at a magnetic first-order phase transition. It vanishes at very low temperatures $T < 1$ K along the nearly horizontal phase line $H = H_c$ of the metamagnetic transition. Tentatively, the lower bound of the corresponding coexistence region of the AF and PM phases, $H_{c1}(T)$, is located at the kink point of the c_m vs H anomaly (Fig. 3, arrows). The

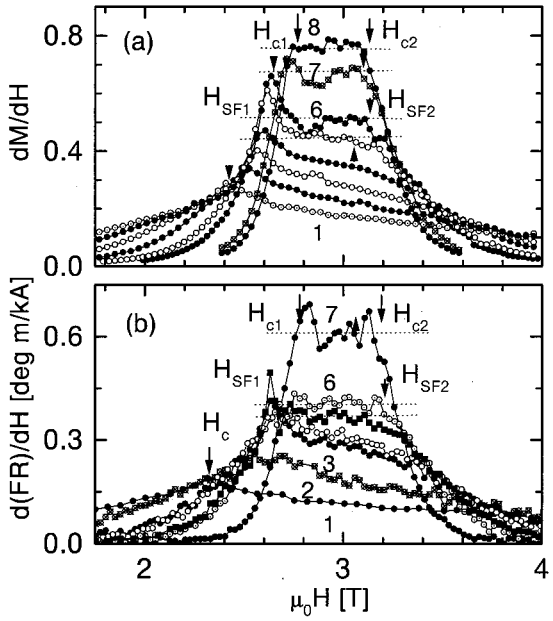

FIG. 4. Field derivatives of the magnetization, dM/dH vs H (a), and of the Faraday rotation, $d(\mathrm{FR})/dH$ vs H (b), recorded at (a) $T=9.0$ K (1), 8.0 K (2), 7.0 K (3), 6.0 K (4), 5.0 K (5), 4.4 K (6), 3.0 K (7), and 2.0 K (8) and (b) 10.0 K (1), 6.1 K (3), 4.9 K (5), and 2.1 K (7) on field increasing and 8.0 K (2), 5.7 K (4), and 4.3 K (6) on field decreasing, respectively. The positions of H_{c1}, H_{c2}, H_{SF1}, H_{SF2}, and H_c are indicated by arrows.

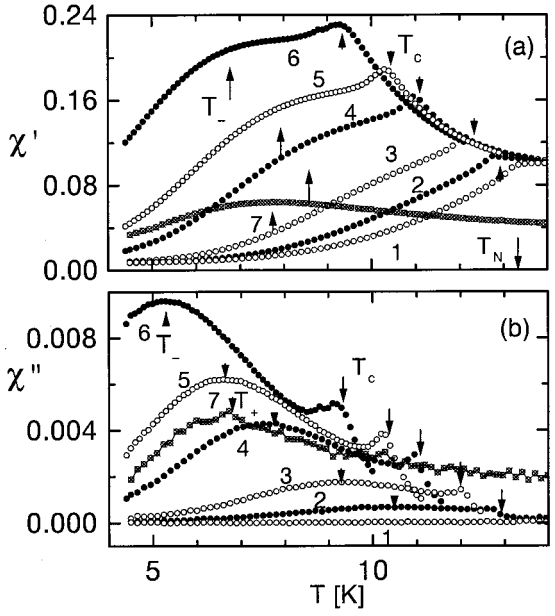

FIG. 5. Susceptibility components χ' vs T (a) and χ'' vs T (b) recorded at $\mu_0 H=0$ T (1), 1.0 T (2), 1.5 T (3), 2.0 T (4), 2.2 T (5), 2.4 T (6), and 3.8 T (7). Anomaly temperatures T_-, T_+, T_N, and T_c are indicated by arrows.

broad anomaly at higher fields referring to the upper anomaly line, $H_+(T)$,[4,5] shifts towards lower fields on cooling and seems to merge into $H_{c2}(T)$ at the upper bound of the AF+PM coexistence region.

Figure 4 shows derivatives of isothermal magnetization curves, dM/dH vs H (a), recorded within $2 \leqslant T \leqslant 9$ K. The peaks observed at $T>5$ K [Fig. 4(a), arrow at curve 1] designate the critical field $H_c(T)$ in perfect agreement with the c_m data [Fig. 1(b), open squares]. At low temperatures (curves 7 and 8), the susceptibility dM/dH maximizes and behaves plateau like as expected for a first-order metamagnetic transition between the boundary values H_{c1} and H_{c2} of the mixed AF+PM phase [Fig. 1(b), crosshatched squares]. The levels of curves 7 and 8 are smaller than expected, $dM/dH \approx 1/N \approx 1.1$ ($N=$demagnetization factor), since the transverse components of the AFI phase reduces the effective susceptibility. The situation changes for $T_e \approx 3.5\,\mathrm{K} < T < T_m \approx 5$ K, where a sharp peak at H_{SF1} and the upper edge of the subsequent plateau at H_{SF2} define the lower and upper bounds of a new ''spin-flop-like'' (SF) phase [Fig. 1(b), crosshatched diamonds]. At $T \approx 6$ K the horizontal part of the dM/dH plateau starts to shrink as a consequence of the bending down of the second-order upper phase boundary towards the MCP, where it meets the two first-order (H_1 and H_{SF1}) and one second-order (H_c) phase boundaries.

The SQUID magnetometric results are confirmed by use of FR. By probing very small sample volumes via a pinhole of about 50 μm diameter, blurring effects of concentration gradients are overcome. As a consequence, e.g., a considerable increase of the H_{SF1} peak is encountered at $T=4.9$ K [Fig. 4(b), curve 5, solid squares].

The new ''spin-flop-like'' phase contrasts with a classic one, since the magnetization, when extrapolated to zero, does not hit the field axis at $H=0$. We presume this to be related to the nearby AFI and AFII phases, which both possess transverse AF spin components. The different phases meeting at the MCP might be described by the order parameters L_a, L_t, M_a, and M_t, where L, M, a, and t designate AF, FM, axial, and transverse, respectively. In analogy with $FeBr_2$,[1] we propose all of the four order parameters to exist in the ''parent'' phase AFI, while in the two ''daughter'' phases with transverse ordering $L_t \neq 0$, either $M_t \equiv 0$ (AFII) or both $M_t \equiv 0$ and $L_a \equiv 0$ (SF). In the PM phase all order parameters but the induced one, M_a, vanish.

The peaks in the isomagnetic ac susceptibility curves, χ' and χ'' vs T in Figs. 5(a) and 5(b), respectively, reveal values of $H_c(T)$ (arrows), which fit well with the phase diagram for $\mu_0 H \leqslant 2.4$ T [Fig. 1(b), crosses]. Here $T_c(H=0)=13.05$ K is in good agreement with the caloric value of $T_N=13.15$ K (Fig. 2). Large anomalies (arrows) for $\mu_0 H \leqslant 2.4$ T are due to noncritical fluctuations at $H_-(T)$, while the flat peak observed at $\mu_0 H=3.8$ T refers to $H_+(T)$ [Fig. 1(b), tilted cross].

Isothermal ac susceptibility data, χ' vs H [Fig. 6(a)], confirm the static magnetization ones, dM/dH vs H [Fig. 4(a)]. Owing to the finite frequency $f=20$ Hz of the probing field, however, the peaks at H_{SF1} are missing at low temperatures (curves 1 and 2). A slightly rounded peak emerging at higher T characterizes $H_c(T)$. The increase of χ' at $H > H_{\mathrm{SF1}}$ in the SF regime (curves 1 and 2) is tentatively attributed to the low-f dispersion of multidomain states compatible with the

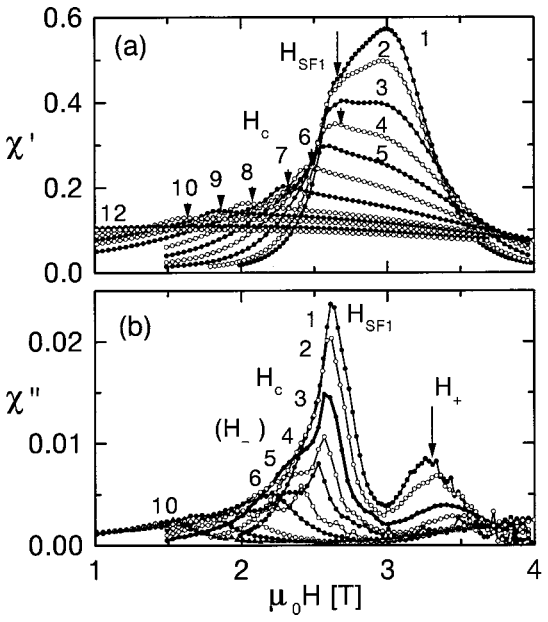

FIG. 6. Susceptibility components χ' (a) and χ'' vs $\mu_0 H$ (b) recorded at $T=4.4$ K (1), 5.0 K (2), 6.0 K (3), 7.0 K (4), 8.0 K (5), 9.0 K (6), 10.0 K (7), 11.0 K (8), 11.5 K (9), 12.0 K (10), 13.0 K (11), and 14.0 K (12). Anomaly fields H_c, H_{SF1}, H_-, and H_+ are indicated.

sixfold degeneracy of L_t. The values of H_{SF1}, H_c, and H_+ are corroborated by well-resolved peaks of χ'' vs H [Fig. 6(b), open and solid diamonds in Fig. 1(b)].

Our investigations show that small amounts of nonmagnetic impurities have drastic consequences on the magnetic behavior of the parent compound $FeBr_2$. First of all, when subjected to axial magnetic fields, $Fe_{0.95}Mg_{0.05}Br_2$ exhibits a crossover from three-dimensional random exchange to RF Ising model behavior. This manifests itself in a change of the critical behavior of the specific heat from an asymmetric λ shape at $H=0$ to a perfectly symmetric semilogarithmic one $c_m \propto \log_{10}|T/T_c-1|$ at $\mu_0 H \approx 1.8$ T.[7] Dynamic rounding[7] occurs at higher fields until no anomaly is any longer observed at $\mu_0 H > 2.25$ T.

Remarkably, the anomaly at $H_1(T)$, being due to transverse spin ordering, is not affected by the longitudinal RF's. This explains its sharp appearance in the high-field range $\mu_0 H \approx 2.5$ T in both c_m vs T (Fig. 2) and c_m vs H (Fig. 3). Obviously, much more entropy is spent at the AFI-to-AFII than at the AFII-to-PM transition. As conjectured previously,[1] the AFI-to-AFII transition is very probably due to a strong increase of the transverse AF ordering accompanied by the loss of the weak ferromagnetic transverse moment. One of the driving mechanisms is assumed to be the symmetric nondiagonal exchange interaction, which is allowed by symmetry in the trigonal point group of $FeBr_2$. However, as pointed out by Mukamel[8] and verified explicitly for $FeBr_2$,[1] its contribution to the free energy vanishes in the case of a $\mathbf{q}=0$ Néel-type ground state. Thus the appearance of the $H_1(T)$ phase line in pure $FeBr_2$ is still a puzzle.[1]

Tentatively, we propose that unavoidable defects like stacking faults, which seem to be quite frequent in $FeBr_2$-like systems,[9] break the translation symmetry in real samples of $FeBr_2$ and thus activate the nondiagonal exchange to a certain extent. This tendency will be enhanced in a random solid like $Fe_{0.95}Mg_{0.05}Br_2$. We propose, hence, the strong anomalies at $H_1(T)$ to be due to the loss of the threefold rotational symmetry, which makes nondiagonal exchange effective. Since this mechanism virtually lowers the anisotropy of the system, even spin-flop-like transitions become possible in the low-T range. This is in our opinion the second drastic effect of the magnetic dilution on the $FeBr_2$ system. Beyond the transition line $H_{SF1}(T)$, hence, strong axial susceptibility is encountered before the system reaches the PM regime at $H_{SF2}(T)$.

Unusually and not predicted by the mean-field theory of conventional anisotropic Heisenberg antiferromagnets,[10] a metamagnetic regime evolves from the canted AFI phase at lowest temperatures. Clearly, more thorough research of this SF phase and its adjacent critical points (CEP and MCP) seems highly desirable. In particular, it will be interesting to confirm these conjectures in future neutron scattering experiments.

Ch.B., W.K., and O.P. gratefully appreciate the hospitality of RIKEN (Japan) and thank H. Junge for crystal growth and DFG for financial support. The work done in Japan was supported by Grants-in-Aid from the Japanese Ministry of Education, Science, Sports and Culture and from the Hayashi Memorial Foundation for Female Natural Scientists.

*On leave of absence from the Department of Physics, Tokyo Institute of Technology, Japan.

[1] Ch. Binek, T. Kato, W. Kleemann, O. Petracic, D. Bertrand, F. Bourdarot, P. Burlet, H. Aruga Katori, K. Katsumata, K. Prokes, and S. Welzel, Eur. Phys. J. B **15**, 35 (2000).

[2] J. M. Kincaid and E. G. D. Cohen, Phys. Rep., Phys. Lett. **22C**, 57 (1975).

[3] E. Stryjewski and N. Giordano, Adv. Phys. **26**, 487 (1977).

[4] M. M. P. de Azevedo, Ch. Binek, J. Kushauer, W. Kleemann, and D. Bertrand, J. Magn. Magn. Mater. **140–144**, 1557 (1995).

[5] H. Aruga Katori, K. Katsumata, and M. Katori, Phys. Rev. B **54**, R9620 (1996).

[6] W. Selke, Z. Phys. B **101**, 145 (1996); M. Pleimling and W. Selke, Phys. Rev. B **56**, 8855 (1997); K. Held, M. Ulmke, N. Blümer, and D. Vollhardt, *ibid.* **56**, 14 469 (1997); M. Pleimling, Eur. Phys. J. B **10**, 465 (1999); M. Acharyya, U. Nowak, and K. D. Usadel, Phys. Rev. B **61**, 464 (2000).

[7] For a review, see D. P. Belanger and A. P. Young, J. Magn. Magn. Mater. **100**, 272 (1991).

[8] D. Mukamel, Phys. Rev. Lett. **46**, 845 (1981).

[9] See, e.g., A. Ito and N.-L. Di, J. Phys. Soc. Jpn. **68**, 1098 (1999); recent γ-ray diffraction data [Ch. Binek, T. Kato, and H. Hünnefeld (unpublished)] are in favor of a superstructure along the c axis in $FeBr_2$.

[10] I. Vilfan and S. Galam, Phys. Rev. B **34**, 6428 (1986).